NUCL SCI TECH (2017) 28:32
DOI 10.1007/s41365-017-0194-y

Electronic structure and optical properties of the scintillation material wurtzite ZnS(Ag)

Dong-Yang Jiang[1] · Zheng Zhang[1] · Rui-Xue Liang[2] · Zhi-Hong Zhang[1] · Yang Li[1] · Qiang Zhao[1] · Xiao-Ping Ouyang[1,3,4]

Received: 12 June 2016 / Revised: 30 August 2016 / Accepted: 8 September 2016 / Published online: 31 January 2017

Abstract In order to investigate the effect of Ag doping (ZnS(Ag)) and Zn vacancy (V_{Zn}) on the alpha particle detection performance of wurtzite (WZ) ZnS as a scintillation cell component, the electronic structure and optical properties of ZnS, ZnS(Ag), and V_{Zn} were studied by first-principle calculation based on the density functional theory. The results show that the band gaps of ZnS, ZnS(Ag), and V_{Zn} are 2.17, 1.79, and 2.37 eV, respectively. Both ZnS(Ag) and V_{Zn} enhance the absorption and reflection of the low energy photons. A specific energy, about 2.9 eV, leading to decrease of detection efficiency is observed. The results indicate that Ag doping has a complex effect on the detection performance. It is beneficial to produce more visible light photons than pure WZ ZnS when exposed to the same amount of radiation, while the increase of the absorption to visible light photons weakens the detection performance. Zn vacancy has negative effect on the detection performance. If we want to improve the detection performance of WZ ZnS, Ag doping will be a good way, but we should reduce the absorption to visible light photons and control the number of Zn vacancy rigorously.

Keywords Wurtzite ZnS · Electronic structure · Optical properties · First-principle

1 Introduction

In recent years, the zinc sulfide (ZnS) crystal has been a research focus due to its attractive physical properties [1–4] as well as its promising device applications [5–12]. It has been widely used in diverse fields including semiconductors, thin-film electroluminescent, and sensors. Silver-activated ZnS (ZnS(Ag)) has a maximum in the scintillation emission spectrum at 450 nm. The light conversion efficiency is relatively poor for fast electrons which may be an advantage when detecting heavy charged particles in a relatively intense γ-ray background [13]. ZnS(Ag) can also be used to detect thermal neutrons if a lithium compound enriched in ^{6}Li is incorporated [14]. Another use for ZnS(Ag) is for the detection of fast neutrons [15]. A fast neutron detector can be made by imbedding the ZnS(Ag) in a clear hydrogenous compound. ZnS is usually used as a scintillation cell component for the detection of the alpha particles [16–20].

There are two types of structures of ZnS, the wurtzite (WZ) structure and the zinc-blende (ZB) structure. There are a few researchers that made contributions to the study of WZ ZnS. Chen et al. [21] investigated the optical and

This work was supported by the National Natural Science Foundation of China (Nos. 11275071 and 11305061), the Fundamental Research Funds for the Central Universities (Nos. 2014MS53 and 2014ZZD09), and the Student's Platform for Innovation and Entrepreneurship Training Program of North China Electric Power University (No. 15129).

✉ Qiang Zhao
qzhao@ncepu.edu.cn

[1] Beijing Key Laboratory of Passive Safety Technology for Nuclear Energy, School of Nuclear Science and Engineering, North China Electric Power University, Beijing 102206, China

[2] School of Electrical and Electronic Engineering, North China Electric Power University, Beijing 102206, China

[3] Northwest Institute of Nuclear Technology, Xi'an 710024, China

[4] School of Materials Science and Engineering, Xiangtan University, Xiangtan 411105, China

excitonic properties of the ZnS nanowires toward efficient ultraviolet emission at room temperature. Reddy et al. [22] found that WZ ZnS is more desirable for optoelectronics because its luminescent properties are considerably more enhanced than sphalerite. Zeng et al. [23] investigated charge transfer and optical properties of wurtzite-type $ZnS/(CdS/ZnS)_n (n = 2, 4, 8)$ superlattices. Zhang et al. [24] investigated the blue and green emissions of ZnS ceramics and found that the wurtzite-type ZnS ceramics could provide an interesting application in the development of novel luminescent devices. Ong et al. [25] determined optical constants of WZ ZnS thin films by spectroscopic ellipsometry. Zhang et al. [26] researched the surface states and their influence on the luminescence of ZnS nanocrystallite. Ye et al. [27] investigated the origin of the green photoluminescence for the ZnS. Tadashi Mitsui et al. [28] studied the cathodoluminescence image of defects and luminescence centers in ZnS/GaAs(100). Wang et al. [29] studied the photovoltaic effect of ZnS as semiconductors.

However, there are few theoretical researches on the ZnS as a scintillation cell component, and many researchers [16–20] studied the ZnS crystal as a kind of scintillation material used for alpha particles detection through the experimental study, but they did not mention the crystal structure of the ZnS crystal. As a scintillation component, the electronic structure and optical properties are important to detective performance. In order to explain the mechanism of the scintillation luminescence in WZ ZnS, we need to know the effect of the Ag doping, Zn vacancy on the detective performance of ZnS, and whether the WZ crystal structure is better as a kind of scintillation material. We studied the lattice constants, electronic structure, and optical properties of the pure ZnS, ZnS(Ag), and V_{Zn}.

2 Calculation

The space group of WZ ZnS is P63mc(186), and the crystal structure of the perfect WZ ZnS is shown in Fig. 1a, b. There is one zinc atom and one sulfur atom in each ZnS unit cell, in which the atomic coordinate of Zn is (0.3333, 0.6667, 0), and the atomic coordinate of S is (0.3333, 0.6667, 0.374). We applied a $2 \times 2 \times 1$ supercell to calculating the electronic structure and optical properties of ZnS, ZnS(Ag), and V_{Zn}. Figure 1c is the crystal structure of the ZnS doped with an Ag atom, noted as ZnS(Ag). Figure 1d shows the crystal structure of the ZnS with a Zn vacancy, noted as V_{Zn} in this paper. The Ag doping concentration and the vacancy concentration may be a bit high, but it is reasonable to explain the effects of the Ag doping and the vacancy on the electronic structure and the optical properties of the WZ ZnS.

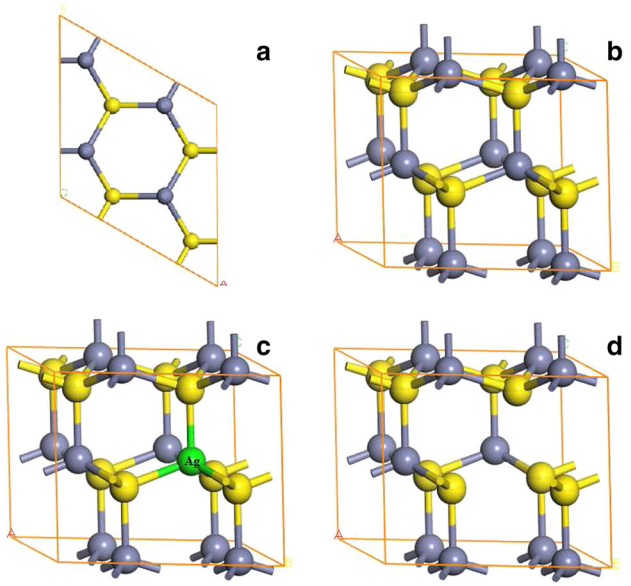

Fig. 1 The supercell structure of WZ ZnS, ZnS(Ag), and V_{Zn} (The *yellow* balls represent S, *gray* balls represent Zn, and *green* ball represents Ag): **a** the top view of ZnS, **b** the three views ZnS, **c** ZnS(Ag), **d** V_{Zn}. (Color figure online)

All calculations were completed by using the Cambridge Serial Total Energy Package (CASTEP) [30]. CASTEP is an ab initio quantum mechanics application software based on the DFT. It uses the plane wave pseudo-potential (PWP) method to substitute ionic potentials. The expansion of the electronic wave function is spread through the plane wave basis sets. The exchange correlation potentials among the electrons are described by the general gradient approximation (GGA) with a Perdew–Burke–Ernzerhof (PBE) form [31]. To ensure the calculation efficiency and accuracy, after the convergence test, we chose the kinetic cutoff energy as 400 eV for all the calculations, and the *k*-mesh as $4 \times 4 \times 4$. We obtained the equilibrium crystal structure when the maximum force on all atoms was <0.05 eV/nm, the maximum stress of the crystal was smaller than 0.02 GPa, and the maximum change of energy per atom was 1.0×10^{-5} eV/atom. The valence electrons involved are $3d^{10}4s^2$ for Zn, $3s^23p^4$ for S, and $4d^{10}5s^1$ for Ag, respectively. After we optimized the crystal structure of ZnS, ZnS(Ag), and V_{Zn}, we calculated the electronic structure and optical properties of them.

3 Results and discussion

3.1 Optimization of the crystal structure

In order to figure out the electronic structure and optical properties of WZ ZnS, ZnS(Ag), and V_{Zn}, we optimized those crystal structures first. Table 1 shows the results of

Table 1 The equilibrium lattice parameters and band gaps of WZ ZnS, ZnS(Ag), and V_{Zn}

Crystal	ZnS^{Exp} [1, 38]	ZnS [32, 39]	ZnS	ZnS(Ag)	V_{Zn}
a (Å)	3.822	3.840	3.841	3.853	3.790
c (Å)	6.260	6.267	6.303	6.397	6.345
Band gap (eV)	3.7–3.8	2.19	2.17	1.79	2.37

our calculation, the other theoretical results, and experimental data.

From Table 1, lattice parameters of those crystals that we calculated are consistent with the other theoretical results and experimental data. The band gap of WZ ZnS we calculated is 2.17 eV which is consistent with other theoretical values 2.19 eV [32], 2.06 eV [33], while they are smaller than the experimental data 3.7–3.8 eV [1] and 3.91 eV [34] for the WZ ZnS. The underestimation of the band gaps is mainly due to the simple form of GGA, and this is a well-known issue [35]. It should be noted that the density functional formalism is limited in its validity [36] so the band structure derived from it cannot be used directly for comparison with experiment. However, GGA is still a widely used method and has achieved many successes. Results based on GGA are generally acclaimed [37].

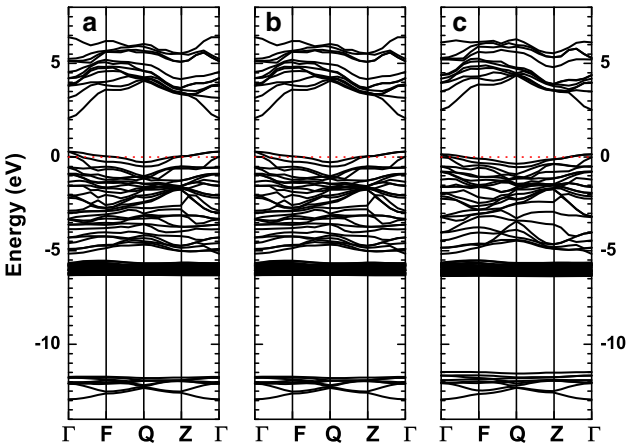

Fig. 2 Band structure of WZ ZnS, ZnS(Ag), and V_{Zn}: **a** ZnS, **b** ZnS(Ag), **c** V_{Zn}

3.2 Electronic structure

As a scintillation material, the electronic structure of WZ ZnS is important to its luminescence performance. When ZnS is exposed to the alpha particles radiation, photons are produced by the de-excitation of the electrons. The luminescence performance properties of scintillation materials are closely related to the electronic structure of them. The detection performance will be better with higher luminous efficiency of the visible light photons. We calculated the band structure and the electronic density of states of ZnS, ZnS(Ag), and V_{Zn}.

Figure 2 is the band structure of those crystals, which shows the band gaps of WZ ZnS, ZnS(Ag), and V_{Zn} are 2.17, 1.79, and 2.37 eV, respectively. Compared with the pure ZnS, ZnS(Ag) changes somewhat because of the doping. The conduction band of ZnS(Ag) is similar to that of ZnS, but the top point of the valence band of ZnS(Ag) moves to a higher energy level. Both the top point of the valence band and the lowest point of the conduction band of V_{Zn} move to a higher energy level when compared with ZnS. The top point of the valence band of V_{Zn} is still lower than that of ZnS(Ag).

In a word, the main changes occur near the Fermi level when there are Ag doping and Zn vacancy in WZ ZnS. The electrons of ZnS(Ag) need less energy to transit from the valence band to conduction band. Therefore, Ag doping can improve the detection efficiency of ZnS because it can produce more photons when exposed to the same amount of nuclear radiation and their energy is in the visible light range. On the contrary, the electrons of V_{Zn} need more energy, which means that Zn vacancy decreases the detection efficiency of ZnS.

Figure 3 is the distribution of the total density of states (TDOS) of WZ ZnS, ZnS(Ag), and V_{Zn}. From Fig. 3, the result of the TDOSs is in agreement with the band structure. In the low valence band (−13 to 11 eV), no changes occur. The lowest point of the conduction band changes somewhat in ZnS(Ag) and V_{Zn}. Those results can explain the difference of the band gaps.

Figure 4 shows the TDOS and the partial density of states (PDOS) of WZ ZnS. The low valence band of ZnS is composed by the *s* state electrons of S, and the high valence band is mainly composed by the d state electrons of Zn and *p* states electrons of S. The formation of the conduction band is the contribution of the *s* state electrons of Zn and the *p* state electrons of S.

Figure 5 shows the TDOS and PDOSs of ZnS(Ag). The top point of the valence band of ZnS(Ag) moves to a higher energy level, and the lowest point of the conduction band does not change. The *s* state electrons of Ag make some contribution to the high valence band, the *d* state electrons of Ag make some contribution to the conduction band, and the result is the band gap becomes smaller than that of pure ZnS. Compared with the pure ZnS crystal, Ag doping could produce more visible light photons when ZnS(Ag) is exposed to the same amount of radiation.

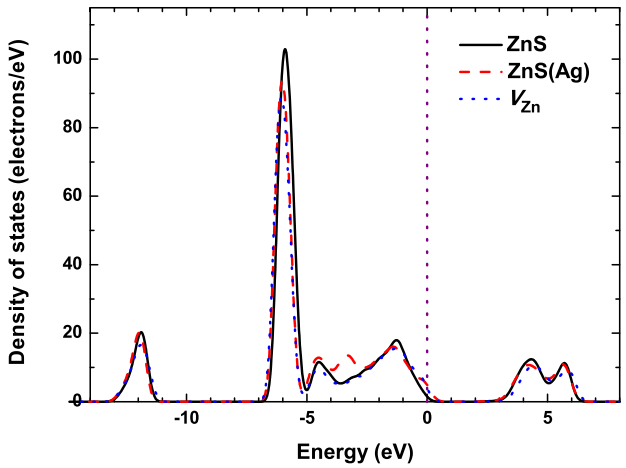

Fig. 3 TDOS of WZ ZnS, ZnS(Ag), and V_{Zn}

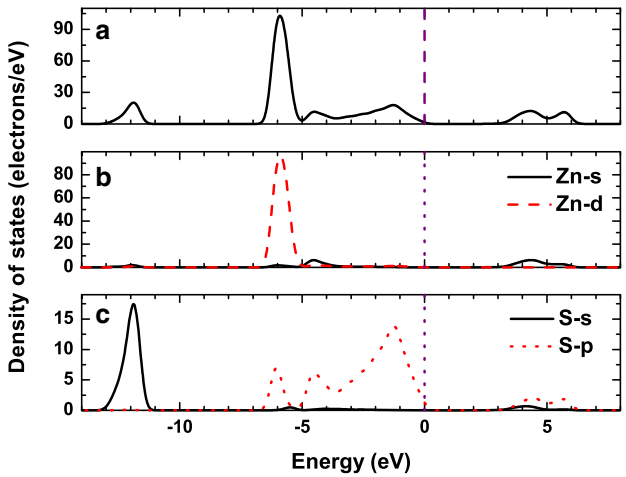

Fig. 4 TDOS and PDOS of WZ ZnS, **a** TDOS of ZnS, **b** and **c** PDOS of WZ ZnS

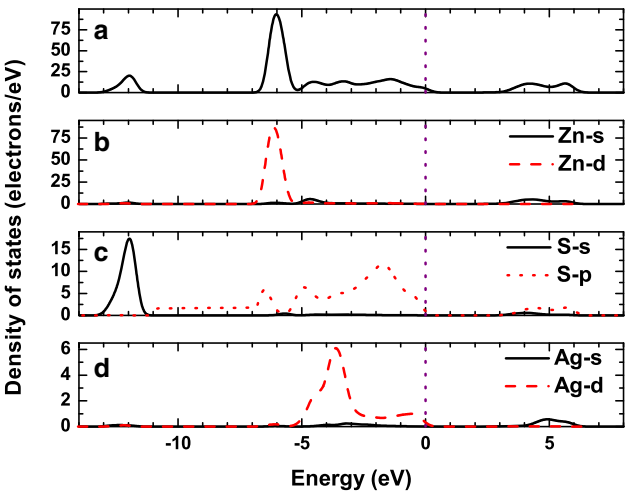

Fig. 5 TDOS and PDOS of ZnS(Ag), **a** TDOS of ZnS(Ag), **b** and **c** PDOS of ZnS(Ag)

Figure 6 shows the TDOS and PDOSs of V_{Zn}. Both the top point of the valence band and the lowest point of the conduction band of V_{Zn} move to a higher energy level when compared with WZ ZnS. The band gap of V_{Zn} is bigger than that of ZnS, which means electrons need more energy to transit from the valence band to the conduction band. This result decreases the detection efficiency. Therefore, reducing Zn vacancies is beneficial to improving the detective performance of ZnS.

3.3 Optical properties

In the linear response range, the optical response function of a crystal can usually be described by a dielectric function in a complex number form $\varepsilon(\omega) = \varepsilon_1(\omega) + i\varepsilon_2(\omega)$, from which we can easily get the spectrum information. The imaginary part, $\varepsilon_2(\omega)$, represents absorption characteristic well, and it is associated electronic structure. We calculated $\varepsilon_2(\omega)$ according to the definition of direct probability transition.

Figure 7 shows $\varepsilon_2(\omega)$ of WZ ZnS, ZnS(Ag), and V_{Zn}, respectively. In the high energy range (5–10 eV), the change is not obvious. In the low energy, about 1.5 eV, there are two peaks belonging to ZnS(Ag) and V_{Zn}, respectively. Those changes indicate that Ag doping and Zn vacancy can enhance the absorption of the ZnS crystal to the low energy photons, and it has a negative effect on the detection efficiency of ZnS(Ag) and V_{Zn}.

Figure 8 shows the absorption spectra of ZnS, ZnS(Ag), and V_{Zn}. Obviously, Ag doping and Zn vacancy could increase the absorption of low energy photons whose energy is in the visible light range. V_{Zn} absorbs more photons than ZnS(Ag) at the same energy.

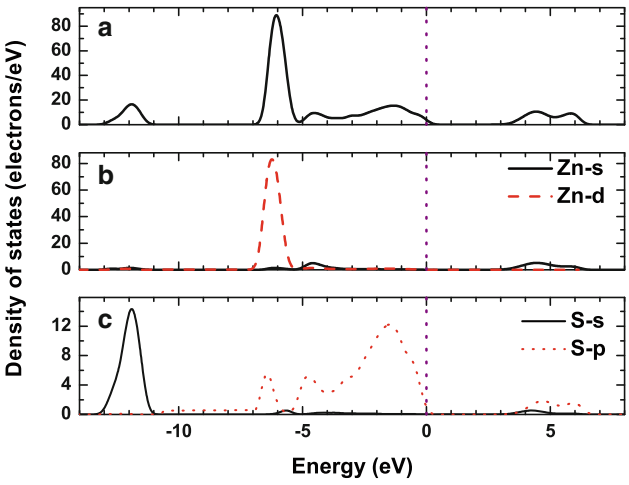

Fig. 6 TDOS and PDOS of V_{Zn}, **a** TDOS of V_{Zn}, **b** and **c** PDOS of V_{Zn}

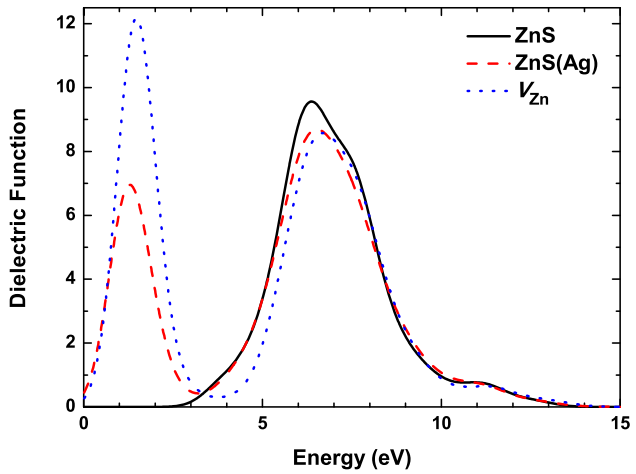

Fig. 7 The imaginary part of dielectric function of WZ ZnS, ZnS(Ag), and V_{Zn}

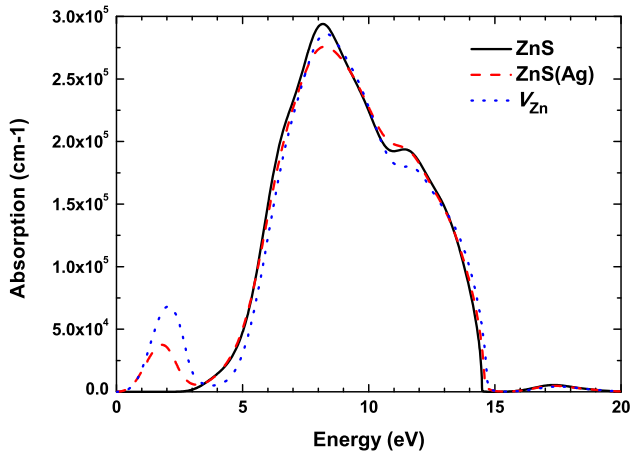

Fig. 8 Absorption coefficient of ZnS, ZnS(Ag), and V_{Zn}

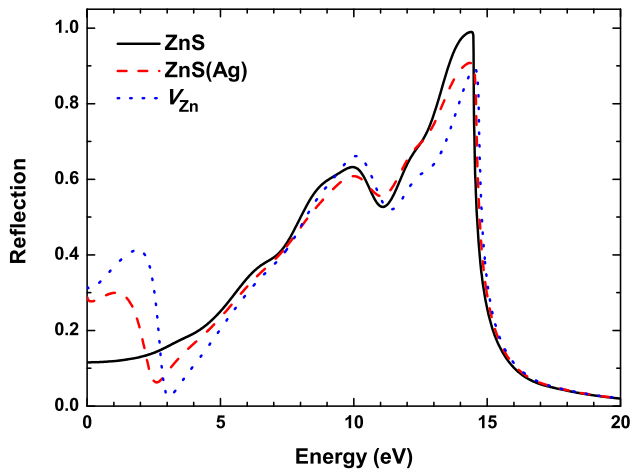

Fig. 9 Reflection coefficient of ZnS, ZnS(Ag), and V_{Zn}

Figure 9 shows the reflection coefficient of WZ ZnS, ZnS(Ag), and V_{Zn}. In the low energy range, around 1.8 eV, we can observe two peaks belonging to ZnS(Ag) and V_{Zn}, respectively. They are beneficial to detective performance. Valleys appear around the 2.9 eV where the reflection coefficients of ZnS(Ag) and V_{Zn} are smaller than the perfect ZnS. The valleys would weaken the detection efficiency. In short, a red shift can be observed in Fig. 9. Ag doping and Zn vacancy increase the reflection coefficient of the low energy photons. A higher reflection coefficient of the low energy photons can improve the detection efficiency of ZnS.

4 Summary

In order to investigate the effect of Ag doping and Zn vacancy on the detective performance of WZ ZnS as a scintillation cell component, we calculated the electronic structure and optical properties of ZnS, ZnS(Ag), and V_{Zn} by using the first-principle calculation method based on the DFT. The results of our calculation are as follows:

1. The band gaps of WZ ZnS, ZnS(Ag), and V_{Zn} are 2.17, 1.79, and 2.37 eV, respectively. It shows that electrons of ZnS(Ag) need less energy, and electrons of V_{Zn} need more energy than ZnS, to transit from the valence band to conduction band when they are exposed to the same amount of radiation.
2. The density of states shows that the top point of the valence band of ZnS(Ag) moves to a higher energy level, the lowest point of the conduction band does not change, and the result is the band gap becomes smaller than pure WZ ZnS. Both the top point of the valence band and the lowest point of the conduction band of V_{Zn} move to a higher energy level, when compared with pure ZnS.
3. Ag doping and Zn vacancy enhance the absorption of the low energy photons, especially in V_{Zn}. Reflection coefficient of ZnS(Ag) and V_{Zn} perform higher than ZnS in the visible light range. Meanwhile, a specific energy, about 2.9 eV, leading to decrease of detection efficiency is observed, which needs to be avoided.

The results indicate that Ag doping has a complex effect on the detection performance. It is beneficial to produce more visible light photons than pure WZ ZnS when exposed to the same amount of radiation, because the increase of the absorption to visible light photons weakens the detection performance. Zn vacancy has a negative effect on the detection performance. If we want to improve the detection performance of WZ ZnS, Ag

doping will be a good way, but we should reduce the absorption to visible light photons and control the number of vacancy carefully.

References

1. B.Y. Geng, X.W. Liu, Q.B. Du et al., Structure and optical properties of periodically twinned ZnS nanowires. Appl. Phys. Lett. **88**, 163104 (2006). doi:10.1063/1.2196827
2. N. Kubota, M. Katagiri, K. Kamijo, Evaluation of Zns-family phosphors for neutron detectors using photon counting method. Nucl. Instrum. Methods A **529**, 321–324 (2004). doi:10.1016/j.nima.2004.05.004
3. J. Schrier, D.O. Demchenko, A.P. Alivisatos, Optical properties of ZnO/ZnS and ZnO/ZnTe heterostructures for photovoltaic applications. Nano Lett. **2007**(7), 2377–2382 (2007). doi:10.1021/nl071027k
4. J.H. Li, X.H. Zeng, Z.H. Ji et al., Electronic structure and optical properties of Ag-doping and Zn vacancy impurities in ZnS. Acta Phys. Sin. **60**, 607–613 (2011). doi:10.1016/j.pmatsci.2010.10.001
5. X. Fang, T. Zhai, K. Gautam et al., ZnS nanostructures: from synthesis to applications. Prog. Mater. Sci. **56**, 175–287 (2011). doi:10.1016/j.pmatsci.2010.10.001
6. J. Xie, First-principles study on the magnetism in ZnS-based diluted magnetic semiconductors. J. Magn. Magn. Mater. **322**, L37–L41 (2010). doi:10.1016/j.jmmm.2010.04.031
7. X. Fang, Y. Bando, M. Liao et al., Single-crystalline Zns nanobelts as ultraviolet-light sensors. Adv. Mater. **21**, 2034–2039 (2009). doi:10.1002/adma.200802441
8. J.H. Yu, J. Joo, H.M. Park et al., Synthesis of quantum-sized cubic ZnS nanorods by the oriented attachment mechanism. J. Am. Chem. Soc. **127**, 5662–5670 (2005). doi:10.1021/ja044593f
9. X.S. Fang, C.H. Ye, L.D. Zhang et al., Temperature controlled catalytic growth of Zns nanostructures by the evaporation of Zns nanopowders. Adv. Funct. Mater. **15**, 63–68 (2005). doi:10.1002/adfm.200305008
10. Z. Wang, L.L. Daemen, Y. Zhao et al., Morphology-tuned wurtzite-type ZnS nanobelts. Nat. Mater. **15**, 922–927 (2005). doi:10.1038/nmat1522
11. Y. Zhao, Y. Zhang, H. Zhu et al., Low-temperature synthesis of hexagonal (wurtzite) ZnS nanocrystals. J. Am. Chem. Soc. **126**, 6874–6875 (2004). doi:10.1021/ja048650g
12. N. Gao, W. Chen, R. Zhang et al., First principles investigation on the electronic, magnetic and optical properties of Bi0.8M0.2Fe0.9Co0.1O3 (M= La, Gd, Er, Lu). Comput. Theor. Chem. **1084**, 36–42 (2016). doi:10.1016/j.comptc.2016.03.001
13. W.G. Moulton, C.W. Sherwin, Fast neutron detector. Rev. Sci. Instrum. **33**, 361–362 (1949). doi:10.2172/4396836
14. R. Stedman, Scintillator for thermal neutrons using Li^6F and ZnS(Ag). Rev. Sci. Instrum. **31**, 1156 (1960). doi:10.1063/1.1716833
15. P.G. Koontz, G.R. Keepin, J.E. Ashley, ZnS(Ag) phosphor mixtures for neutron scintillation counting. Rev. Sci. Instrum. **26**, 352–356 (1955). doi:10.2172/4394603
16. J.S. Mccloy, M. Bliss, B. miller et al., Scintillation and luminescence in transparent colorless single and polycrystalline bulk ceramic ZnS. J. Lumin. **157**, 416–423 (2015). doi:10.1016/j.jlumin.2014.09.015
17. M. Ardid, J.L. Ferrero, A. Herrero, Study of the background on a ZnS(Ag) alpha counter with a plastic veto detector. Nucl. Instrum. Methods A **557**, 510–515 (2006). doi:10.1016/j.nima.2005.10.124
18. Y. Morishita, S. Yamamoto, K. Izaki et al., Performance comparison of scintillators for alpha particle detectors. Nucl. Instrum. Methods A **764**, 383–386 (2014). doi:10.1016/j.nima.2014.07.046
19. H. Philipsborn, Large-area low-level gross alpha ZnS scintillation counting. Appl. Radiat. Isot. **67**, 797–799 (2009). doi:10.1016/j.apradiso.2009.01.020
20. L. Pujol, J.A. Suarez-Navarro, M. Montero, A method for the selection of the optimum counting conditions in a ZnS(Ag) scintillation detector. Appl. Radiat. Isot. **52**, 891–897 (2000). doi:10.1016/s0969-8043(99)00139-6
21. R. Chen, D. Li, B. Liu et al., Optical and excitonic properties of crystalline ZnS nanowires: toward efficient ultraviolet emission at room temperature. Nano Lett. **10**, 4956–4961 (2010). doi:10.1021/nl102987z
22. D.A. Reddy, D.H. Kim, S.J. Rhee et al., Tunable blue-green-emitting wurtzite ZnS: Mg nanosheet-assembled hierarchical spheres for near-UV white LEDs. Nanoscale Res. Lett. **9**, 1–8 (2014). doi:10.1186/1556-276X-9-20
23. X. Zeng, W. Zhang, J. Cui et al., Charge transfer and optical properties of wurtzite-type $ZnS/(CdS/ZnS)_n (n = 2, 4, 8)$ superlattices. Mater. Res. Bull. **50**, 359–364 (2014). doi:10.1016/j.materresbull.2013.11.010
24. W. Zhang, X.H. Zeng, H.F. Liu et al., Synthesis and investigation of blue and green emissions of ZnS ceramics. J. Lumin. **134**, 498–503 (2013). doi:10.1016/j.jlumin.2012.07.039
25. H.C. Ong, R.PH Chang. Optical constants of wurtzite ZnS thin films determined by spectroscopic ellipsometry. Appl. Phys. Lett. **79**, 3612–3614 (2001). doi:10.1063/1.1419229
26. X.B. Zhang, H.W. Song, L.X. Yu et al., Surface states and its influence on luminescence in ZnS nanocrystallite. J. Lumin. **118**, 251–256 (2006). doi:10.1016/j.jlumin.2005.07.003
27. C.H. Ye, X.S. Fang, G.H. Li et al., Origin of the green photoluminescence from zinc sulfide nanobelts. Appl. Phys. Lett. **85**, 3035–3037 (2004). doi:10.1063/1.1807018
28. T. Mitsui, N. Yamamoto, T. Tadokoro et al., Cathodoluminescence image of defects and luminescence centers in ZnS/GaAs (100). J. Appl. Phys. **80**, 6972–6979 (1997). doi:10.1063/1.363770
29. K. Wang, J. Chen, Z. Zeng et al., Synthesis and photovoltaic effect of vertically aligned ZnO/ZnS core/shell nanowire arrays. Appl. Phys. Lett. **96**(12), 123105 (2010). doi:10.1063/1.3367706
30. M.C. Payne, M.P. Teter, C. Allan et al., Iterative minimization techniques for ab initio total-energy calculations: molecular dynamics and conjugate gradients. Rev. Mod. Phys. **64**, 1045–1097 (1992). doi:10.1103/revmodphys.64.1045
31. J.P. Perdew, K. Burke, M. Ernzerhof, Generalized gradient approximation made simple. Phys. Rev. Lett. **77**, 3865–3868 (1996). doi:10.1103/physrevlett.77.3865
32. E.H. Cui, Y.Z. Zhao, C. Yan et al., First-principles calculations for electronic, optical and thermodynamic properties of ZnS. Chin. Phys. B **17**, 3867–3874 (2008). doi:10.1088/1674-1056/17/10/053
33. B. Gilbert, B.H. Frazer, H. Zhang et al., X-ray absorption spectroscopy of the cubic and hexagonal polytypes of zinc sulfide. Phys. Rev. B. **66**, 245205 (2002). doi:10.1103/PhysRevB.66.245205
34. A. Goldmann, W. Gudat, O. Rader, *Electronic Structure of Solids: Photoemission Spectra and Related Data* (Springer, New York, 1994)
35. J.P. Perdew, S. Kurth, A. Zupan et al., Accurate density functional with correct formal properties: a step beyond the generalized gradient approximation. Phys. Rev. Lett. **82**, 2544 (1999). doi:10.1103/PhysRevLett.82.2544

36. G. Onida, L. Reining, A. Rubio, Electronic excitations: density-functional versus many-body Green's-function approaches. Rev. Mod. Phys. **74**, 601 (2002). doi:10.1103/RevModPhys.74.601
37. R.O. Jones, Density functional theory: Its origins, rise to prominence, and future. Rev. Mod. Phys. **87**, 897 (2015). doi:10.1103/RevModPhys.87.897
38. Q. Li, C. Wang, Fabrication of wurtzite ZnS nanobelts via simple thermal evaporation. Appl. Phys. Lett. **83**, 359–361 (2003). doi:10.1063/1.1591999
39. O. Zakharov, A. Rubio, X. Blase et al., Quasiparticle band structures of six II-VI compounds: ZnS, ZnSe, ZnTe, CdS, CdSe, and CdTe. Phys. Rev. B **50**, 10780–10787 (1994). doi:10.1103/physrevb.50.10780